

# New high-precision orbital and physical parameters of the double-lined low-mass spectroscopic binary BY Draconis

K. G. Hełminiak,<sup>1,2\*</sup> M. Konacki,<sup>1,3</sup> M. W. Muterspaugh,<sup>4,5</sup> S. E. Browne,<sup>6</sup>  
A. W. Howard<sup>7</sup> and S. R. Kulkarni<sup>8</sup>

<sup>1</sup>Department of Astrophysics, Nicolaus Copernicus Astronomical Center, ul. Rjabiańska 8, 87-100 Toruń, Poland

<sup>2</sup>Departamento de Astronomía y Astrofísica, Pontificia Universidad Católica, Casilla 306, Santiago, Chile

<sup>3</sup>Astronomical Observatory, A. Mickiewicz University, ul. Słoneczna 36, 60-286 Poznań, Poland

<sup>4</sup>Department of Mathematics and Physics, College of Arts and Sciences, Tennessee State University, Boswell Science Hall, Nashville, TN 37209, USA

<sup>5</sup>Center of Excellence in Information Systems, Tennessee State University, 3500 John A. Merritt Blvd., Box No 9501, Nashville, TN 37203-3401, USA

<sup>6</sup>Experimental Astrophysics Group, Space Sciences Laboratory, University of California, 7 Gauss Way, Berkeley, CA 94720, USA

<sup>7</sup>UC Berkeley Astronomy Department, Campbell Hall MC 3411, Berkeley, CA 94720, USA

<sup>8</sup>Division of Physics, Mathematics and Astronomy, California Institute of Technology, Pasadena, CA 91125, USA

Accepted 2011 September 8. Received 2011 September 7; in original form 2010 June 28

## ABSTRACT

We present the most precise to date orbital and physical parameters of the well-known short period ( $P = 5.975$  d), eccentric ( $e = 0.3$ ) double-lined spectroscopic binary BY Draconis (BY Dra), a prototype of a class of late-type, active, spotted flare stars. We calculate the full spectroscopic/astrometric orbital solution by combining our precise radial velocities (RVs) and the archival astrometric measurements from the Palomar Testbed Interferometer (PTI). The RVs were derived based on the high-resolution echelle spectra taken between 2004 and 2008 with the Keck I/high-resolution echelle spectrograph, Shane/CAT/HamSpec and TNG/SARG telescopes/spectrographs using our novel iodine-cell technique for double-lined binary stars. The RVs and available PTI astrometric data spanning over eight years allow us to reach 0.2–0.5 per cent level of precision in  $M\sin^3i$  and the parallax but the geometry of the orbit ( $i \simeq 154^\circ$ ) hampers the absolute mass precision to 3.3 per cent, which is still an order of magnitude better than for previous studies. We compare our results with a set of Yonsei–Yale theoretical stellar isochrones and conclude that BY Dra is probably a main-sequence system more metal rich than the Sun. Using the orbital inclination and the available rotational velocities of the components, we also conclude that the rotational axes of the components are likely misaligned with the orbital angular momentum. Given BY Dra’s main-sequence status, late spectral type and the relatively short orbital period, its high orbital eccentricity and probable spin–orbit misalignment are not in agreement with the tidal theory. This disagreement may possibly be explained by smaller rotational velocities of the components and the presence of a substellar mass companion to BY Dra AB.

**Key words:** techniques: interferometric – techniques: radial velocities – binaries: spectroscopic – binaries: visual – stars: fundamental parameters – stars: individual: (BY Dra).

## 1 INTRODUCTION

Regular studies of BY Draconis (BY Dra) (Gl 719, HD 234677, HIP 91009, NLTT 46684 and BD+51 2402) started in mid-1940s when Münch noted the calcium H and K lines to be in emission (Münch 1944). This fact was later confirmed by Popper (1953) who also noted strong emission Balmer series lines. In one of his

spectrograms the emission was particularly strong which led to a conclusion that BY Dra may be a member of a new group of flare stars (Popper 1953). Photometric monitoring was then carried out (e.g. Masani, Broglia & Pestarion 1955) but the variability was not confirmed until 1966 when Chugainov obtained a quasi-sinusoidal light curve with an amplitude of 0.23 mag and a period of 3.826 d (Chugainov 1966), later interpreted as a rotation of a spotted star (Krzemiński 1969). No flares were then observed. The first photometric flares were reported by Cristaldi & Rodono (1968) who later observed 12 flares that occurred between 1967 July and

\*E-mail: xysiek@ncac.torun.pl

1970 July (Cristaldi & Rodono 1970,1971). Krzemiński (1969) confirmed the sinusoidal variability with an  $\sim 3.826$  d period and noted the variation of its amplitude. Many subsequent studies of BY Dra's variability have been carried out and the most up-to-date value of the rotational period  $P_{\text{rot}} = 3.8285$  d is given by Pettersen, Olah & Sandmann (1992) as an average period for their entire 1965–1989 data set.

The double-lined spectroscopic nature was revealed by Krzemiński & Kraft (1967). They announced a period of 5.981 d but never published their full orbital solution. It was done later by Bopp & Evans (1973) on the basis of 23 spectra taken between 1966 June and 1971 July at the Hale and McDonald observatories, 15 of which showed unblended Ca II H and K lines. Bopp & Evans (1973) also performed an analysis of the spots on the surface of BY Dra and estimated the rotational velocity of the primary (spotted) component to be  $\sim 5$  km s $^{-1}$  and the (rotational) inclination to be  $\sim 30^\circ$ . Since then BY Dra became a prototype of a new class of stars characterized by a late type, brightness variation caused by spots, rapid rotation and strong emission in H and K lines. The short orbital period also seems to be a characteristic for most of BY Dra-type stars (Bopp, Noah & Klimke 1980).

The orbital solution was later improved by Vogt & Fekel (1979) on the basis of high-resolution reticon spectra. Vogt & Fekel (1979) also found the projected rotational velocity of the primary to be 8.5 km s $^{-1}$  under the assumption of the rotational inclination being the same as the orbital one (spin–orbit alignment). They estimated the radius of the primary to be greater than  $0.9 R_\odot$  which led to a conclusion that BY Dra was a pre-main-sequence system. This conclusion was supported by the large brightness ratio despite the mass ratio being close to 1 ( $q = 0.98$ ), the Barnes–Evans visual surface brightness relation (Barnes, Evans & Moffet 1978) and the inequality of the rotational and orbital periods. However, the assumption of the spin–orbit alignment in close binary systems was later criticized in several works, e.g., Głęboccki & Stawikowski (1995). The orbital parameters as well as the value of the projected rotational velocities for both components were shortly after improved by Lucke & Mayor (1980). They used new measurements from CORAVEL and obtained rotational velocities  $v_1 \sin i = 8.05$  and  $v_2 \sin i = 7.42$  km s $^{-1}$  and the mass ratio  $q = 0.89$  significantly more different from 1 than that of Vogt & Fekel (1979). They also estimated the magnitude difference (1.15 mag) and the primary's radius (1.2–1.4  $R_\odot$ ) but noted that a higher macroturbulence velocity would reduce the radius estimation by a factor of 2.

The most up-to-date spectroscopic orbital solution was given together with the first astrometric solution by Boden & Lane (2001). They combined the archival radial velocity (RV) measurements with the visibility-based ( $V^2$ ) astrometric measurements obtained with the Palomar Testbed Interferometer (PTI; Colavita et al. 1999) in 1999. Their orbital inclination ( $152^\circ$ , retrograde orbit) agrees with the first estimations of the rotational inclination (Bopp & Evans 1973) but not with the later ones (Głęboccki & Stawikowski 1995).

Finally, it is worth noting that BY Dra is a hierarchical multiple system. A common proper-motion companion was found by Zuckerman et al. (1997) about 16.7 arcsec to the northeast of the primary. From the visual and infrared photometry of BY Dra C they also deduced that this component is a normal M5 dwarf at least  $3 \times 10^8$  yr old which makes the pre-main-sequence nature of BY Dra less probable. Yet another putative component is reported in the *Hipparcos* Double and Multiple System Annex (Perryman 1997). A photocentric circular orbital solution with a period of 114 d and  $113^\circ$  inclination is reported. Boden & Lane (2001) however demonstrated that this is an improbable solution since the fourth body would pro-

duce significant perturbations to the BY Dra AB RVs but no such periodicity is seen in the archival RVs.

We spectroscopically observed BY Dra over the years 2004–2008 using a combination of high-resolution echelle spectrographs (HIRES) (10-m Keck I), SARG (3.5-m TNG) and HamSpec (3-m Shane telescope) as a part of our ongoing RV search for circumbinary planets (Konacki et al. 2009, 2010). Even though we knew that BY Dra was too variable to allow us to reach an RV precision sufficient to detect planets, it was nevertheless observed to make use of an extensive and publicly available set of PTI  $V^2$  measurements spanning now over eight years.

In this paper, we present a new orbital solution and the orbital and physical parameters of the BY Dra AB binary, derived with a precision of over an order of magnitude better than by Boden & Lane (2001). Thanks to our superior iodine-cell-based RVs and the full set of PTI visibilities we are able to put strong constraints on the nature of the system. In Sections 2 and 3 we present the data –  $V^2$ s and RVs. In Section 4 we describe their modelling. The results of our data modelling are presented in Section 5 and the state of BY Dra is then discussed in Section 6.

## 2 VISIBILITIES

Often the main observable in the interferometric observations at optical or infrared wavelength is the normalized amplitude of the coherence function – a fringe pattern contrast, commonly known as the visibility (squared,  $V^2$ ) of the interferometric fringes, calculated by definition as follows (Boden 2000):

$$V^2 = \left( \frac{I_{\text{max}} - I_{\text{min}}}{I_{\text{max}} + I_{\text{min}}} \right)^2, \quad (1)$$

where  $I_{\text{max}}$  and  $I_{\text{min}}$  are the maximum and minimum intensity of the fringe pattern, respectively. For a given object the observed  $V^2$  depends on its morphology and the projected baseline vector of a two-aperture interferometer  $\mathbf{B}_\perp$  on to a plane tangent to the sky. For binaries,  $V^2$  also varies due to the orbital motion of the components. In the case of a binary, approximated by two uniform discs, the squared visibility can be modelled as follows (see e.g. Boden 2000):

$$V_{\text{binary}}^2 = \frac{V_1^2 + r^2 V_2^2 + 2r V_1 V_2 \cos(2\pi \mathbf{B}_\perp \cdot \Delta \mathbf{s} / \lambda)}{(1 + r)^2}, \quad (2)$$

where  $V_{1,2}$  are the visibilities of uniform discs (components) of the angular diameters  $\theta_1$  and  $\theta_2$  and are calculated as follows:

$$V_i^2 = \left( \frac{2J_1(\pi\theta_i B_\perp \lambda)}{\pi\theta_i B_\perp \lambda} \right)^2; \quad i = 1, 2; B_\perp = \|\mathbf{B}_\perp\|, \quad (3)$$

where  $r$  is the brightness ratio at the observing wavelength  $\lambda$ ,  $J_1(x)$  is the first-order Bessel function and  $\Delta \mathbf{s} = (\Delta\alpha, \Delta\delta)$  is the separation vector between the primary and the secondary in the plane tangent to the sky. This vector is related to the Keplerian orbital elements, orbital period  $P$ , eccentric anomaly  $E$  (from the Kepler equation  $E - e \sin E = M$ ) and the parallax  $\kappa$  in the usual way (van de Kamp 1967).

A visibility measurement needs to be calibrated by observing at least one calibration source before or after a target observation. The calibrator is typically a single star with a known diameter and its visibility  $V_{\text{cal}}^2$  is given by relation (3). The correction factor  $f$  which should be applied to the observed target  $V^2$  is simply the ratio  $f = V_{\text{cal}}^2 / V_{\text{cal-meas}}^2$ , where  $V_{\text{cal-meas}}^2$  is the measured calibrator visibility. The 'true' target visibility is then

$$V_{\text{true}}^2 = f V_{\text{measured}}^2. \quad (4)$$

**Table 1.** Absolute values of the RVs of BY Dra with their errors and the best-fitting  $O - Cs$ . The formal error is denoted with  $\sigma$  and the adopted final error with  $\epsilon$ . The subscript ‘1’ is for the primary and ‘2’ for the secondary. K/H denotes the measurements from Keck I/HIRES, T/S from TNG/SARG and S/H from Shane/HamSpec.

TDB-2400000	$v_1$ (km s <sup>-1</sup> )	$\sigma_1$ (km s <sup>-1</sup> )	$\epsilon_1$ (km s <sup>-1</sup> )	$O - C_1$ (km s <sup>-1</sup> )	$v_2$ (km s <sup>-1</sup> )	$\sigma_2$ (km s <sup>-1</sup> )	$\epsilon_2$ (km s <sup>-1</sup> )	$O - C_2$ (km s <sup>-1</sup> )	Tel./Spec.
53 276.214 636	-49.472 97	0.006 68	0.150 15	0.052 36	1.742 03	0.011 62	0.150 45	-0.041 17	K/H
53 276.218 251	-49.298 37	0.008 22	0.150 22	0.067 79	1.578 02	0.013 71	0.150 63	-0.024 14	K/H
53 276.274 388	-46.622 69	0.009 94	0.150 33	0.148 84	-1.240 54	0.011 93	0.150 47	0.108 49	K/H
53 276.277 251	-46.469 12	0.010 18	0.150 34	0.164 44	-1.392 94	0.011 52	0.150 44	0.113 03	K/H
53 276.371 688	-41.654 63	0.009 90	0.150 33	0.193 86	-6.807 59	0.017 58	0.151 03	0.141 39	K/H
53 276.381 066	-41.160 56	0.009 34	0.150 29	0.193 69	-7.393 37	0.026 63	0.152 35	0.117 82	K/H
53 276.383 829	-41.016 84	0.010 20	0.150 35	0.191 38	-7.571 52	0.029 20	0.152 82	0.105 79	K/H
53 328.260 862	-34.238 94	0.010 17	0.150 34	-0.130 33	-15.800 64	0.011 63	0.150 45	-0.001 87	K/H
53 329.192 929	-55.694 33	0.009 58	0.150 31	-0.365 69	8.161 17	0.011 85	0.150 47	-0.198 37	K/H
53 567.417 144	-37.512 57	0.007 65	0.150 19	-0.074 42	-12.244 47	0.014 09	0.150 66	-0.235 57	K/H
53 654.287 570	-2.810 22	0.007 07	0.150 17	-0.264 82	-51.636 84	0.012 57	0.150 53	0.042 75	K/H
53 655.270 877	-8.628 44	0.008 67	0.150 25	-0.209 46	-44.964 07	0.007 76	0.150 20	0.050 11	K/H
53 656.250 010	-21.534 47	0.014 34	0.150 68	0.294 88	-29.897 13	0.029 74	0.152 92	-0.129 65	K/H
54 191.188 978	-13.366 07	0.021 68	0.151 56	0.101 01	-39.927 90	0.033 36	0.153 66	-0.103 95	T/S
54 192.164 756	-2.954 88	0.013 36	0.150 59	-0.108 36	-52.028 01	0.030 54	0.153 08	-0.103 39	T/S
54 247.147 226	-12.621 61	0.020 67	0.151 42	-0.030 78	-40.662 18	0.027 48	0.152 50	0.195 85	T/S
54 275.086 679	-7.541 49	0.012 98	0.150 56	0.039 06	-46.516 56	0.025 29	0.152 12	0.009 09	T/S
54 281.357 833	-3.424 39	0.021 36	0.151 51	0.189 14	-50.407 87	0.023 44	0.151 82	0.029 77	S/H
54 290.431 083	-38.188 61	0.005 94	0.150 12	-0.181 64	-11.424 22	0.009 05	0.150 27	-0.062 82	K/H
54 290.596 520	-41.902 39	0.008 05	0.150 22	-0.078 12	-7.000 27	0.012 80	0.150 55	0.016 60	K/H
54 727.249 888	-52.872 36	0.016 49	0.150 90	-0.092 39	5.112 52	0.021 14	0.151 48	-0.362 39	S/H
54 728.248 858	-45.720 92	0.028 49	0.152 68	-0.098 89	-2.562 09	0.020 87	0.151 45	0.075 59	S/H
54 752.198 503	-43.219 49	0.017 16	0.150 98	-0.086 41	-5.074 45	0.016 32	0.150 89	0.394 54	S/H
54 789.116 481	-4.713 13	0.021 99	0.151 60	0.088 52	-49.234 74	0.044 18	0.156 37	-0.149 75	S/H

Uncalibrated visibilities of BY Dra were extracted from the NASA Exoplanet Science Institute (NExSci) Database of the PTI measurements.<sup>1</sup> These measurements were made in the  $K$  (2.2  $\mu\text{m}$ ) and  $H$  (1.6  $\mu\text{m}$ ) bands. They were calibrated using the standard tools provided by NExSci (`getCal` and `wbCalib`). As the calibration objects we used HD 177196 (A7V,  $V = 5.0$  mag,  $K = 4.5$  mag, diameter  $\theta = 0.42$  mas, 6:6 from BY Dra) and HD 185395 (F4V,  $V = 4.5$  mag,  $K = 3.5$  mag,  $\theta = 0.73$  mas, 9:9) as in Boden & Lane (2001). We do not list these measurements as they can be easily obtained using the NExSci Database and tools.

### 3 RADIAL VELOCITIES

Our high-resolution echelle spectra of BY Dra were obtained during 17 nights between 2004 September and 2008 November. We collected 24 spectra using Keck I/HIRES (K/H, 15 spectra), TNG/SARG (T/S, 4) and Shane/HamSpec (S/H, 5) telescopes/spectrographs. Our spectra have the resolutions  $R \sim 67\,000$  for K/H, 86 000 for T/S and 60 000 for S/H. The typical signal-to-noise ratio (SNR) per collapsed pixel at 550 nm was  $\sim 250$  for K/H,  $\sim 90$  for T/S and  $\sim 60$  for S/H. The basic reduction (bias, dark, flat-field, scattered light subtraction) was done with the `CCDRED` and `ECHELLE` packages from `IRAF`.<sup>2</sup> The wavelength solution and RVs were obtained with our novel procedure based on the iodine-cell technique (Konacki 2009; Konacki et al. 2009, 2010). This

procedure employs a tomographic disentangling of the component spectra of double-lined spectroscopic binaries (SB2s) implemented through a maximum entropy method and the two-dimensional cross-correlation technique `TODCOR` (Zucker & Mazeh 1994) using synthetic spectra derived with `ATLAS 9` and `ATLAS 12` codes (Kurucz 1995) as templates for the first approximation of the RVs. With this approach it is possible to reach up to 2 m s<sup>-1</sup> precision in RVs for components of SB2s (Konacki et al. 2009) but in the case of BY Dra the precision is hampered by the activity of the star (presence of spots) and the relatively rapid rotation of both components.

In Table 1 we list our RV measurements together with their uncertainties and the best-fitting  $O - Cs$ . The formal errors,  $\sigma$ , were calculated from the scatter between orders and predominantly reflect a high SNR of our spectra. The formal errors underestimate the true RV scatter (due to activity) and the resulting reduced  $\chi^2$  of the spectroscopic orbital fit was much larger than 1. Hence, to obtain a conservative estimation of the parameters’ errors (and the reduced  $\chi^2$  close to 1) we added in quadrature a systematic error  $\sigma_{\text{sys}}$  of 150 m s<sup>-1</sup>. Let us note that spots can easily induce RV variations at the level of a few hundreds of m s<sup>-1</sup> so the RV variability of BY Dra is not surprising (see e.g. Helminiak & Konacki 2011; Helminiak et al. 2011). We also had to adopt small shifts between each data set as is explained in Konacki et al. (2010). The best-fitting values of the shifts can be found in Table 3 in Section 5. We do not include the CORAVEL data (from Lucke & Mayor 1980) since their precision is substantially worse than ours.

### 4 MODELING

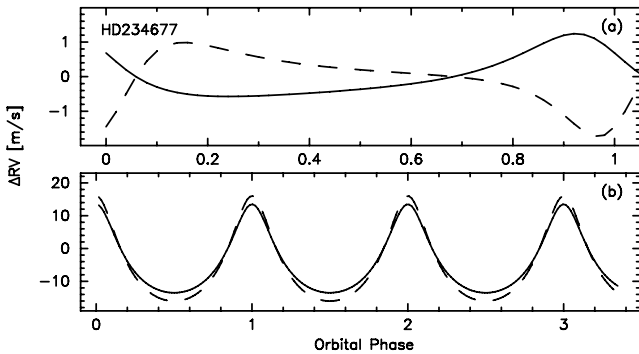
We combined all  $V^2$  and RV measurements in a simultaneous least-squares fit to derive the full orbital solution and the physical parameters of BY Dra. We used our own procedure which minimizes the

<sup>1</sup> <https://nexsciweb.ipac.caltech.edu/pti-archive/secure/main.jsp>

<sup>2</sup> `IRAF` is written and supported by the `IRAF` programming group at the National Optical Astronomy Observatories (NOAO) in Tucson, AZ. NOAO is operated by the Association of Universities for Research in Astronomy, Inc. under cooperative agreement with the National Science Foundation. <http://iraf.noao.edu/>

**Table 2.** Assumed parameters of BY Dra.

Parameter	Primary	Secondary
Effective temperature, $T$ (K)	4000	4000
Potential, $\hat{\Omega}$	24.0	24.5
Synchronization factor, $F$	1.95	1.95
Gravity darkening exponent, $g$	0.3	0.3
Albedo, $A$	0.5	0.5
Apparent diameter, $\theta$ (mas)	0.6	0.5
Metallicity		0.0

**Figure 1.** RV variations of the primary (solid lines) and secondary (dashed lines) stars of BY Dra (HD234677) as a function of the orbital phase. The top panel (a) shows the RV variations due to the tidal distortion of the stars and the bottom panel (b) due to the combined gravitational redshift and transverse Doppler effects which together are the dominant term of the relativistic correction.

$\chi^2$  function with a least-squares Levenberg–Marquardt algorithm. The procedure fits a Keplerian orbit with corrections to the RVs due to tidal distortions of the components and relativistic effects. In order to model the tidal term we use the Wilson–Devinney (WD) code (Wilson & Devinney 1971) as is explained in Konacki et al. (2010) and assume several parameters of BY Dra listed in Table 2. Note that both the relativistic and tidal effects are much smaller than the RV scatter (see Fig. 1) but we decided to include them in the RV model anyway to maintain a consistent treatment of our iodine-cell-based RVs as in Konacki et al. (2010). Apparent stellar diameters were assumed to agree with the estimates of the radii from Section 6.2, since the components are too small and act like point sources.

For a combined  $V^2$ +RV solution our software evaluates the period  $P$ , standard Keplerian elements: major semi-axis  $\hat{a}$  (of B relatively to A – apparent astrometric in mas), inclination  $i$ , eccentricity  $e$ , longitude of pericentre  $\omega$ , longitude of ascending node  $\Omega$ , time of periastron passage  $T_p$ ; velocity amplitudes  $K_1$  and  $K_2$ , systemic velocity  $v_0$ , flux ratios in the observing bands  $r_H$  and  $r_K$ , and a set of shifts in RVs between the two components as well as between the data sets from each telescope/spectrograph. On this basis the software calculates such absolute physical parameters as the absolute major semi-axis  $a_{1,2}$  (relatively to the barycentre – in au), absolute components’ masses  $M_1$  and  $M_2$ , magnitude differences  $\Delta H$  and  $\Delta K$ , and parallax  $\kappa$ . The uncertainty of every parameter is a combination of formal best-fitting least-squares errors and systematic errors as is explained in Konacki et al. (2010). For the systematic errors we assumed the following estimates for additional uncertainties related to the  $V^2$  data reduction: (1) 0.01 per cent in the baseline vector coordinates, (2) 0.5 per cent in  $\lambda$  and (3) 10 per cent in the calibrator and binary component diameters. For the

**Table 3.** Best-fitting orbital solution and its parameters for BY Dra.

Parameter	Value(±)
Orbital solution	
Apparent major semi-axis, $\hat{a}$ (mas)	4.4472(91)
Period, $P$ (d)	5.975 1130(46)
Time of periastron, $T_p$ (TDB-2450000.5)	3999.2144(21)
Eccentricity, $e$	0.300 14(62)
Longitude of periastron, $\omega$ (deg)	230.33(17)
Longitude of ascending node, $\Omega$ (deg)	152.30(10)
Inclination, $i$ (deg)	154.41(29)
Magnitude difference in the $K$ band, $\Delta K$ (mag)	0.530(11)
Magnitude difference in the $H$ band, $\Delta H$ (mag)	0.60(23)
Velocity amplitude, primary, $K_1$ (km s $^{-1}$ )	28.394(60)
Velocity amplitude, secondary, $K_2$ (km s $^{-1}$ )	32.284(61)
Mass ratio, $q$	0.8795(25)
Gamma velocity, $v_0$ (km s $^{-1}$ )	−25.484(46)
Velocity offsets (all in km s $^{-1}$ )	
Secondary versus primary	−0.088(67)
SARG versus HIRES, primary	−0.216(104)
SARG versus HIRES, secondary	−0.343(105)
HamSpec versus HIRES, primary	0.076(83)
HamSpec versus HIRES, secondary	−0.067(85)
Least-squares fit parameters	
Number of RV measurements, total	48
Number of RV measurements, HIRES	30
Number of RV measurements, SARG	8
Number of RV measurements, HamSpec	10
Number of $V^2$ measurements	299
Combined RV rms, prim./sec. (km s $^{-1}$ )	0.169/0.157
Visibilities $V^2$ rms	0.0312
RV $\chi^2$ , primary/secondary	29.17/24.65
Visibilities $V^2$ $\chi^2$	395.3
Degrees of freedom, DOF	330
Total reduced $\chi^2$ , $\chi^2$ /DOF	1.361

**Table 4.** Physical parameters of BY Dra.

Parameter	Primary	Secondary
Major semi-axis, $a$ ( $10^{-2}$ au)	3.4437(73)	3.9155(74)
Major semi-axis, $a$ ( $R_\odot$ )	7.400(16)	8.414(16)
$M \sin^3 i$ ( $M_\odot$ )	0.06387(28)	0.05618(26)
Mass, $M$ ( $M_\odot$ )	0.792(26)	0.697(23)
$M_{K,2MASS}$ (mag)	4.269(21)	4.799(22)
$M_{H,2MASS}$ (mag)	4.420(86)	5.020(149)
Parallax, $\kappa$ (mas)		60.43(12)
Distance, $d$ (pc)		16.548(35)

RVs we assumed (4) 10 per cent in all the parameters from Table 2 except for the temperatures for which we assumed an uncertainty of 2 per cent and for the metallicities we assumed an uncertainty of 0.05 dex.

## 5 RESULTS

The results of our modelling are collected in Tables 3 and 4. Fig. 2 shows our RVs together with the best-fitting orbital solution and the corresponding residuals and their histograms. Fig. 3 shows the same for the PTI  $V^2$  measurements. The resulting astrometric orbit of component B relative to A is shown in panel (d). In Table 3 we show the orbital parameters for BY Dra, the velocity offsets

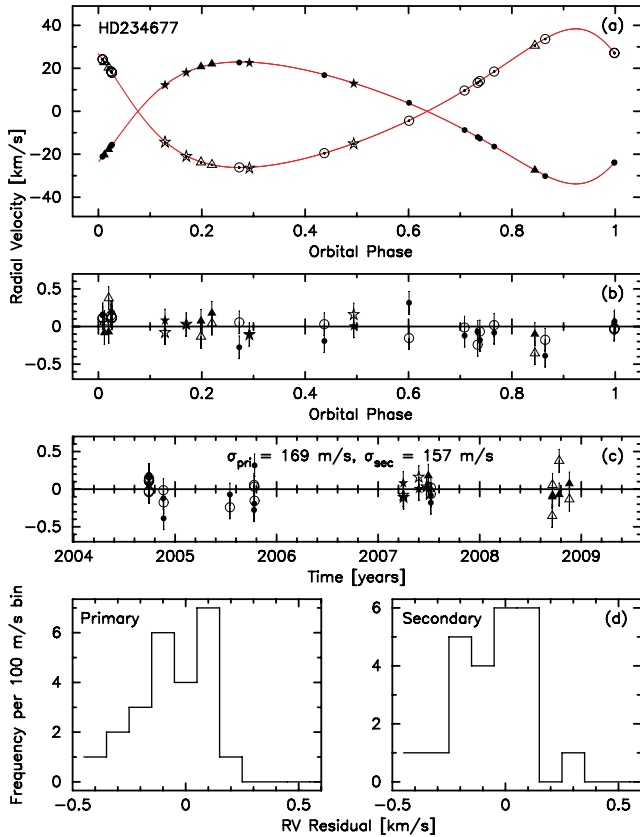


**Figure 2.** Observed and modelled RVs of BY Dra as a function of the orbital phase (a) and their best-fitting residuals as a function of the orbital phase (b) and time (c). The histograms of the residuals for the primary and secondary (d). The Keck I/HIRES measurements are denoted with circles, Shane/CAT/HamSpec with triangles and TNG/SARG with stars.

and other parameters related to the quality of the fit. The absolute physical parameters are listed in Table 4.

As one can see, we were able to reach  $\sim 0.2$  per cent of precision in velocity amplitudes, despite such obstacles as the presence of spots or some rotational broadening of spectral lines. This level of quality has direct implication for the precision of mass ratio  $q$  (0.28 per cent),  $M \sin^3 i$  (0.44 and 0.46 per cent for the primary and secondary, respectively) or major semi-axis ( $\sim 0.2$  per cent both for the apparent and absolute values). The level of precision in  $a$  also proves that the quality of the astrometric solution is very high. The 299 visibility measurements used provide good orbital phase coverage. The apparent and physical values of major semi-axis allow us to determine the parallax, thus the distance to the system, with a precision also close to 0.2 per cent. Our value of the parallax  $-60.43(12)$  mas is in relatively good agreement but almost six times more precise than  $61.15(68)$  mas from the new reduction of the *Hipparcos* data (van Leeuwen 2007). We were also able to precisely derive the magnitude difference in the  $K$  band (282  $V^2$  measurements) but the accuracy for the  $H$  band is much lower due to a lower number of  $V^2$  measurements in  $H$  (only 17).

Our final error in the absolute masses of the BY Dra components is however much higher – 3.3 per cent for both the primary and secondary. This is mainly due to the inclination of the orbit of  $154.4^\circ$ . For such configurations, far from edge-on, a small error in the angle propagates to a large error in the masses. Still it is a considerably more accurate measurement compared to Boden & Lane (2001) of respectively 23 per cent and 25 per cent for the

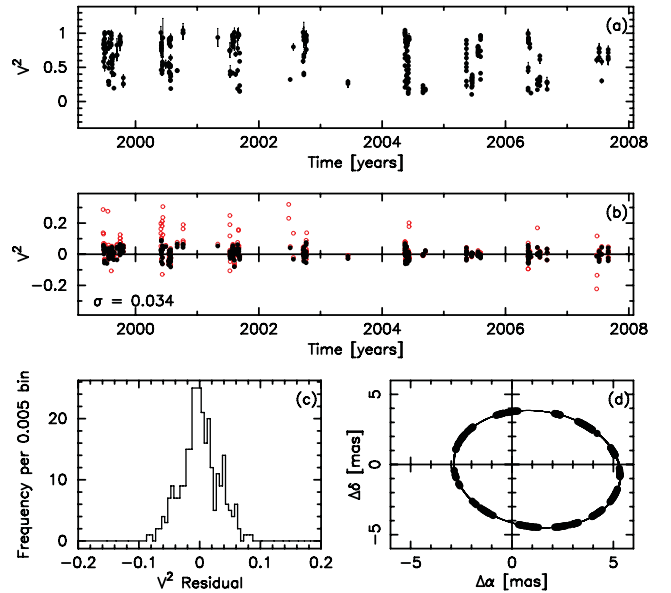


**Figure 3.** Visibility measurements of BY Dra as a function of time (a), and their best-fitting residuals as a function of time (b) and histogram (c). The 299 measurements used to determine the best-fitting orbital solution are denoted with black filled circles. The corresponding orbital coverage and the relative orbit are shown in panel (d).

primary and secondary. This is possible thanks to our superior RV data set (rms of  $\sim 0.15$  versus  $2.3 \text{ km s}^{-1}$ ) and a longer time-span of the astrometric  $V^2$  data.

## 6 DISCUSSION

### 6.1 Age and metallicity

As is pointed out by Torres, Andersen & Giménez (2010), the mass uncertainty should be below 3 per cent to be useful to perform reliable tests of the stellar evolution models. Our precision is close to that but to go below 3 per cent we would require a higher number of precise RVs or more  $V^2$  measurements. Nevertheless, with our measurements we still can place some constraints on the evolutionary properties of BY Dra. We focused on the age estimation to confirm or exclude the pre-main-sequence nature of the system.

We compared our results with the Yonsei–Yale isochrones (Y<sup>2</sup>; Yi et al. 2001; Demarque et al. 2004). We used our estimations of the magnitude differences, parallax and the apparent  $H$  and  $K$  magnitude from Two Micron All Sky Survey (2MASS) (Cutri et al. 2003) to derive the absolute  $H$  and  $K$  magnitudes of each component separately. Using the transformation equations from Carpenter (2001, with updates)<sup>3</sup> we transformed them to the ESO photometric system (van der Bliek, Manfroid & Bouchet 1996), in which the Y<sup>2</sup> isochrones are available. In Fig. 4 we show our measurements in the mass/ $K$ -band (left) and mass/ $H$ -band (right) absolute magnitude diagrams. For comparison we plot the isochrones for ages of 60 Myr (dashed) and 1 Gyr (solid lines) for three values of the metallicity:  $Z = 0.02$  (red), 0.04 (green) and 0.06 (blue). One can see that the properties of the secondary component are not reproduced by the 60 Myr isochrones, which means that it has already settled down on the main sequence. The formally best match is found for  $t = 1$  Gyr and  $Z = 0.04$ . No match was found for ages below 60 Myr for

<sup>3</sup> <http://www.astro.caltech.edu/~jmc/2mass/v3/transformations/>

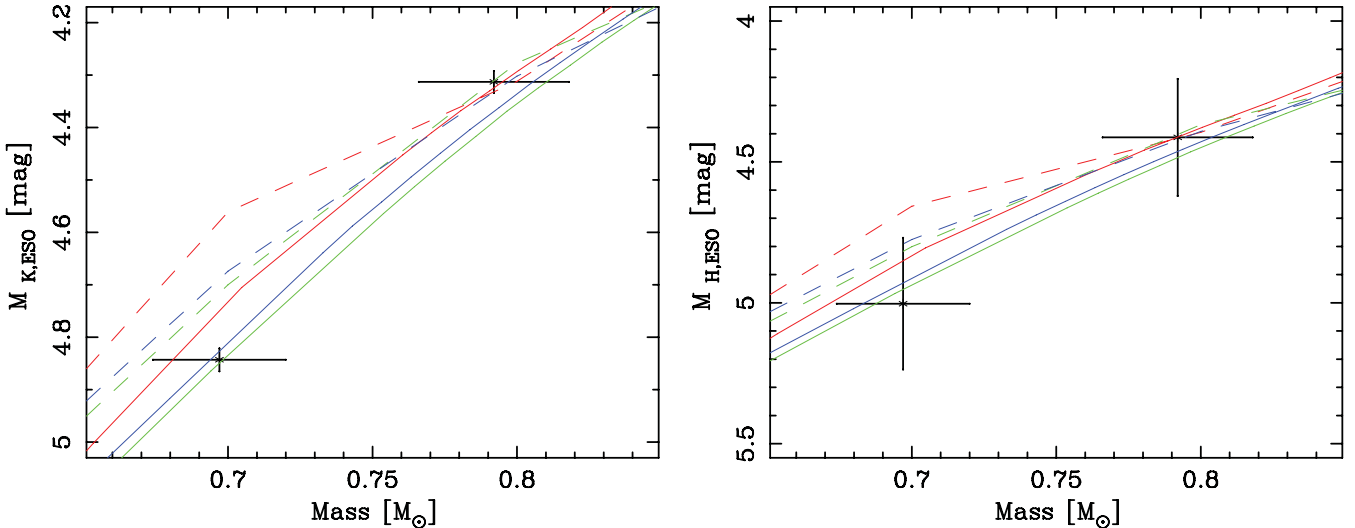


**Figure 4.** Comparison of our results with the Yonsei–Yale isochrones in the mass/*K*-band (left) and mass/*H*-band (right) absolute magnitude (in the ESO system). The isochrones for 1 Gyr are depicted with solid and for 60 Myr with dashed lines. The isochrones for  $Z = 0.02$  are depicted with red, for 0.04 with green and for 0.06 with blue lines.

any  $Z$  value nor for any age value for  $Z < 0.02$ . For  $t > 5$  Gyr only isochrones with metallicities higher than solar reproduce the data points. We thus conclude that BY Dra is probably between 0.2 and 5 Gyr old and is more metal rich than the Sun. The most probable values of age and  $Z$  are 1–2 Gyr and 0.04 respectively. These facts make the pre-main-sequence scenario less probable.

One should notice that the error bars in the masses are enlarged mainly by the uncertainty in the inclination. Any change in  $i$  would shift both components in the same direction – towards higher or lower masses which would definitely not improve the fit. We also have a large uncertainty in  $M_H$ , induced by the error in  $\Delta H$ , which is so large due to a small number of  $V^2$  measurements in this band. Reduction of this uncertainty would allow for putting even more stringent constraints on the nature of the system. At the same time,  $\Delta K$  is very well constrained and shows that the mass ratio  $q \sim 0.88$  is not inconsistent with the observed flux ratio, at least in the *K* band. Using the  $Y^2$  set of isochrones we can estimate that the expected theoretical magnitude difference in  $V$  for the stars having 0.792 and 0.697  $M_\odot$ , should be close to 0.9 mag. This is not in agreement with  $1.15 \pm 0.1$  mag as predicted by Lucke & Mayor (1980). However, given even  $\sim 0.2$  mag variation from spots (Chugainov 1966; Pettersen et al. 1992), we can conclude that such a difference in  $V$  is possible for BY Dra even if it is a main-sequence system.

To put additional constraints on the system’s age, we further calculated the Galactic space velocities  $U$ ,  $V$ ,  $W^4$  relatively to the local standard of rest (Johnson & Soderblom 1987). We applied our values of radial systemic velocity and distance estimation together with proper motion of  $\mu_\alpha = 185.92$  mas yr $^{-1}$  and  $\mu_\delta = -324.81$  mas yr $^{-1}$  from the PPMX catalogue (Röser et al. 2008). Values of  $U = 28.2 \pm 0.1$ ,  $V = -13.16 \pm 0.06$  and  $W = -21.75 \pm 0.10$  km s $^{-1}$  put BY Dra outside of any known young moving group or group candidate (Zhao, Zhao & Chen 2009), and at the transition area between the thin and thick Galactic disc (Bensby, Feltzing &

Lundström 2003; Nordström et al. 2004). This supports the possibility of BY Dra being not a PMS system.

## 6.2 Spin–orbit (mis)alignment

Using the masses and isochrones, we can estimate the radii of each component of BY Dra. In Fig. 5 we plot the  $Y^2$  isochrone for 1 Gyr and  $Z = 0.4$  in a radius/mass plane. As solid horizontal lines we plot the masses together with their uncertainties (dashed lines). Other probable isochrones are very close to the chosen one and do not change the results of our analysis significantly.

Our results predict values of  $R_1 = 0.695 \pm 0.025$  and  $R_2 = 0.61 \pm 0.02$   $R_\odot$ . We can use this together with the rotational velocities and rotational period values from the literature to

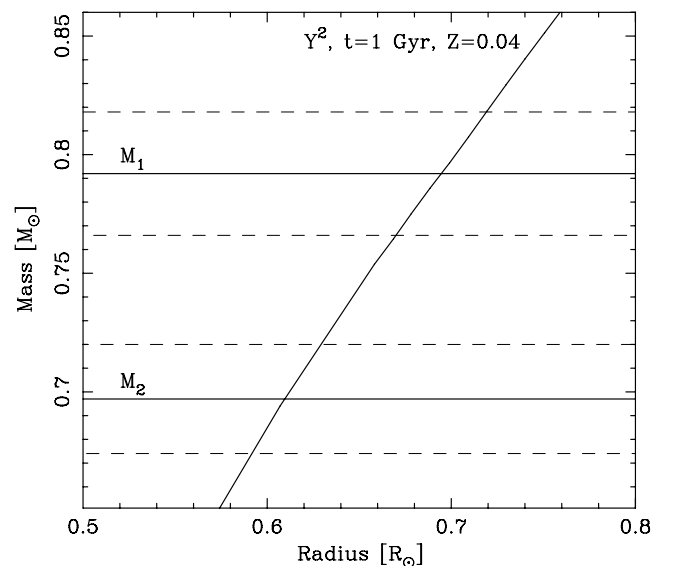


**Figure 5.** Radii of the components as predicted from our estimations of BY Dra’s parameters and the  $Y^2$  best-matching isochrone. Horizontal solid lines represent our estimations of the masses and the dashed lines the  $1\sigma$  ranges of their respective uncertainties.

<sup>4</sup> Positive values of  $U$ ,  $V$  and  $W$  indicate velocities toward the Galactic Centre, direction of rotation and north pole, respectively.

estimate the orbital inclination angles. For this purpose, we use  $v_{\text{rot},1} \sin i_{\text{rot},1} = 8.05 \pm 0.33$  and  $v_{\text{rot},2} \sin i_{\text{rot},2} = 7.42 \pm 1.06 \text{ km s}^{-1}$  from Lucke & Mayor (1980) and  $P_{\text{rot}} = 3.8285 \text{ d}$  from Pettersen et al. (1992). This implies  $R_1 \sin i_{\text{rot},1} = 0.61 \pm 0.03$  and  $R_2 \sin i_{\text{rot},2} = 0.56 \pm 0.08$ . Most of the authors attribute spots to the primary component and refer the  $\sim 3.8 \text{ d}$  period to its rotation. If so, from the values above we can estimate the rotational inclination of the primary to be  $i_{\text{rot},1} = 61^{+12}_{-7}^\circ$  or  $119^{+7}_{-12}^\circ$ . If we assume the secondary to rotate with the given period, we end up with  $i_{\text{rot},2} = 67^\circ$  or  $113^\circ$  and its uncertainties ranging from  $50^\circ$  to  $130^\circ$ . This means that  $i_{\text{rot},2} = 90^\circ$  is also possible. Our results are in good agreement with values given by Głębcki & Stawikowski (1995) who derived  $i_{\text{rot},1} = 60^{+11}_{-9}^\circ$  and  $i_{\text{rot},2} = 85^{+5}_{-15}^\circ$ . None of the values however agrees with the orbital inclination  $i_{\text{orb}} = 154.4^\circ$ . This indicates the spin-orbit misalignment in the BY Dra system. Even if we consider that the theoretical radii are underestimated by about 15 per cent, a well-known issue for late-type stars, we are not able to reproduce the observed  $i_{\text{orb}}$ .

In the case of a spin-orbit alignment, and the literature values of  $v_{\text{rot}} \sin i_{\text{rot}}$ , the radii would have to be  $R_1 \simeq 1.41$  and  $R_2 \simeq 1.30 R_\odot$ . This would occur if the system was  $\sim 3\text{--}4 \text{ Myr}$  old, depending on the metallicity. In such a case both stars should be much brighter in the infrared than it is observed. The predicted  $K$ -magnitudes difference for the two stars would be  $\sim 0.2$  and not  $0.53 \text{ mag}$  which is observed. One would also expect the system to be a member of a young cluster, containing leftovers of the primordial gas, but this is not observed as well.

However, the spin-orbit alignment should be observed for such a close pair of  $\sim 1 \text{ Gyr}$  old stars (Hut 1981). The source of the discrepancy could be for example an overestimated rotational velocity. Głębcki & Stawikowski (1995) in their analysis adopted a value of  $3.6 \text{ km s}^{-1}$ , given by Strassmeier et al. (1993).<sup>5</sup> For this value of  $v_{\text{rot}} \sin i_{\text{rot}}$  we get  $i_{\text{rot},1} \simeq 157^\circ$ , which is very close to the observed orbital inclination. Hence, the spin-orbit alignment may in fact be present in the BY Dra system if Lucke & Mayor (1980) have overestimated their rotational velocity measurements by adopting a too small macroturbulence velocity.

Finally, let us note that a spin-orbit misalignment could manifest itself through its impact on the apsidal precession rate (for a review see Mazeh 2008). Unfortunately, since BY Dra is not an eclipsing system and our RVs and  $V^2$ s are not sufficiently accurate, a measurement of the apsidal motion cannot be carried out. We attempted to fit for  $\dot{\omega}$  but obtained statistically insignificant value.

### 6.3 Rotation pseudo-synchronization

In the case of eccentric orbits one can find a rotational period for which an equilibrium is achieved. This equilibrium, called the *pseudo-synchronization*, occurs when the ratio of the orbital to the rotational period is

$$\frac{P_{\text{orb}}}{P_{\text{rot,ps}}} = \frac{1 + 7.5e^2 + 5.625e^4 + 0.3125e^6}{(1 - e^2)^{3/2}(1 + 3e^2 + 0.375e^4)} \quad (5)$$

(Hut 1981; Mazeh 2008). For the observed eccentricity of BY Dra we get  $P_{\text{orb}}/P_{\text{rot,ps}} = 1.559(3)$  or  $P_{\text{rot,ps}} = 3.833(8) \text{ d}$ , which is in good agreement with the observed  $P_{\text{rot}} = 3.8285 \text{ d}$  and  $P_{\text{orb}}/P_{\text{rot}} = 1.561$ . One may thus conclude that BY Dra is in

a rotational equilibrium. The predicted time-scale of the pseudo-synchronization is in the case of BY Dra similar but slightly shorter than for the spin-orbit alignment (Hut 1981). Using the approximate formula for the synchronization time-scale of late-type stars given by Devor et al. (2008), we get the value of the order of  $10 \text{ Myr}$ , so still smaller than the age of the system. The above equation was however derived for binaries with no additional companions (see below) and the tidal evolution of BY Dra AB might be different if the gravitational influence of the third body is taken into account.

### 6.4 Eccentricity and multiplicity of BY Dra

The eccentricity of BY Dra AB ( $e = 0.3$ ) appears to be unusually high. According to Zahn & Bouchet (1989) a circularization of the orbit of a late-type system such as BY Dra should occur during the pre-main-sequence phase. This was one of the arguments for the PMS nature of BY Dra. Based on Zahn & Bouchet (1989) we can estimate that in the case of BY Dra the eccentricity should drop to a few per cent over  $\sim 10^5 \text{ yr}$ .

However, BY Dra is a hierarchical triple system, with a distant common proper motion companion. The projected separation of  $16.7 \text{ arcsec}$  and our distance determination indicate a projected physical separation of  $277 \text{ au}$ . As estimated by Zuckerman et al. (1997) its mass is about  $0.13 M_\odot$  and assuming a circular orbit, it corresponds to an orbital period of about  $2050 \text{ yr}$ . It is conceivable that the observed eccentricity of the BY Dra AB pair could be explained by the presence of the companion through the Mazeh-Shaham mechanism which results in a cyclic eccentricity variation, known as the Kozai cycles (Kozai 1962; Mazeh & Shaham 1979; Fabrycky & Tremaine 2007; Mazeh 2008).

Let us denote all the orbital and physical parameters of an unknown perturber by the index  $X$ . In order to put some constraints on the properties of the perturber which would induce sufficiently strong Kozai cycles, we followed the analysis of Fabrycky & Tremaine (2007). The two main conditions which have to be met in order to produce the observed eccentricity are: (1) a sufficiently large relative inclination  $i_{\text{rel}}$  of the binary (inner) and the perturber's (outer) orbit; (2) the Kozai cycles time-scale  $\tau$  must be shorter than the period of the inner orbit's pericentre precession. For the BY Dra AB pair the relativistic precession is the dominant one, being at least an order of magnitude faster than any other (tidal or rotational; Fabrycky & Tremaine 2007). The precession period is  $U_{\text{GR}} \simeq 25\,000 \text{ yr}$ , which corresponds to  $\dot{\omega}_{\text{GR}} = 8.0 \times 10^{-12} \text{ rad s}^{-1}$ . Using the formalism of Fabrycky & Tremaine (2007) we can estimate that the observed eccentricity of BY Dra can be induced when  $\tau \dot{\omega}_{\text{GR}}|_{e=0} \leq 2.796$  (in SI units), where the term  $\dot{\omega}_{\text{GR}}$  is computed for  $e = 0$ . From this we can derive the following conditions for the parameters of the perturbing body:

$$P_X^2 \frac{M_1 + M_2 + M_X}{M_X} (1 - e_X^2)^{3/2} < 938.21 \quad (6)$$

or

$$\frac{a_X^3}{M_X} (1 - e_X^2)^{3/2} < 938.21, \quad (7)$$

where the orbital period is given in years, major semi-axis in au and all masses in  $M_\odot$ . The condition  $\tau \dot{\omega}_{\text{GR}}|_{e=0} \leq 2.796$  also allows us to deduce that the relative inclination of the two orbits must be larger than  $78^\circ$  (or smaller than  $102^\circ$ ). This value can be confirmed by the results of Ford, Kozinsky & Rasio (2000), which for the mass ratio of BY Dra AB predict  $i_{\text{rel}} \gtrsim 75^\circ$ . The relatively narrow range of  $i_{\text{rel}}$  allows us to put some useful constraints (which include possible

<sup>5</sup> In fact, in the current version of their catalogue, Strassmeier et al. (1993) cite  $v_{\text{rot}}$  values from Lucke & Mayor (1980).

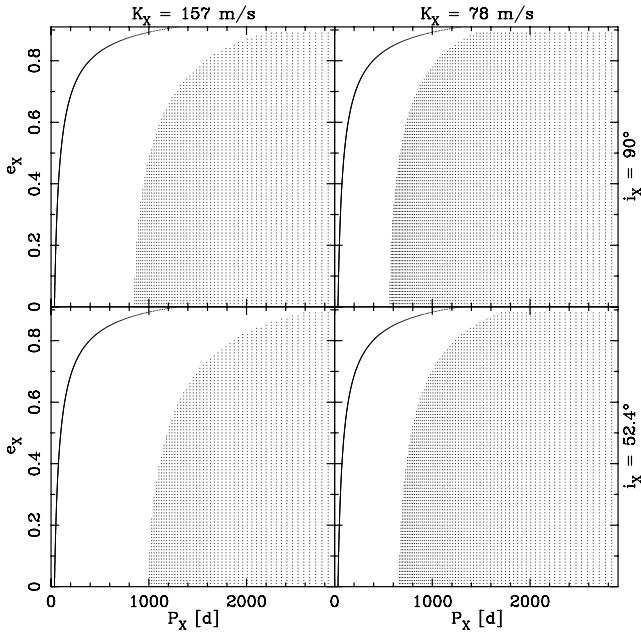


**Figure 6.** Conditions necessary to reproduce the observed eccentricity of BY Dra through the Mazeh–Shaham mechanism by bodies which would produce the RV signal with the semi-amplitude of 157 and 78  $\text{m s}^{-1}$  (the lower rms of the RV orbital solution and half of its value, left-hand and right-hand columns, respectively), and having orbital inclinations of  $90^\circ$  (top row) and  $52.4^\circ$  (bottom row). The shaded areas refer to the periods and eccentricities which would not allow us to induce sufficiently strong Kozai cycles. The lower limit of the period is 35 d (the major semiaxis of 0.24 au) which refers to the shortest stable *circular* orbit (Holman & Wiegert 1999). The area above the solid line corresponds to the eccentric orbits whose periastron distance is within the instability zone (i.e. is shorter than 0.24 au). The upper limit in the eccentricities shown in the figures is 0.9.

values of the longitudes of ascending nodes) on the *absolute* value of the perturber’s orbital inclination:  $i_X \in [52.4, 127.6]$ .

In Fig. 6 we present results of our analysis. We use relation (6) to check whether a body of a certain orbital properties (i.e. period and eccentricity) can produce sufficient Kozai cycles. For the mass  $M_X$  we have taken mass of a body that in an orbit of a given  $P_X$ ,  $e_X$  and  $i_X = 52.4$  or  $90^\circ$  would produce an RV modulation of the inner pair at the level of the smaller rms (157  $\text{m s}^{-1}$ ) or half of that. The four panels show the  $P_X/e_X$  parameter space for the two values of inclinations and RV semi-amplitudes. The shaded areas correspond to the values of  $P_X$  and  $e_X$  for which the observed eccentricity of BY Dra AB would not be induced. The solid line shows the short-period stability border, calculated in such a way that for a given eccentricity the orbit has its periastron at  $\sim 0.24$  au which refers to the smallest stable *circular* orbit (with  $P \simeq 35$  d; Holman & Wiegert 1999). The long-period cut-off at 2900 d is mainly for the clarity, but it is close to double time-span of our observations (1513 d) which means that RV modulations with periods around 3000 d could in principle be detected. The corresponding fourth body detection limits in terms of  $M_X \sin(i_X)$  as a function of its orbital period and eccentricity are presented in Fig. 7.

From those two figures one can deduce that if the observed eccentricity is an effect of the Mazeh–Shaham mechanism, the perturber should be in an orbit of up to single years (major semi-axes from  $\sim 0.2$  to  $\sim 2$  au) and have its mass in the planetary regime. This is consistent with the fact that the interferometric  $V^2$  measurements are fully consistent with a two-disc model, so no additional

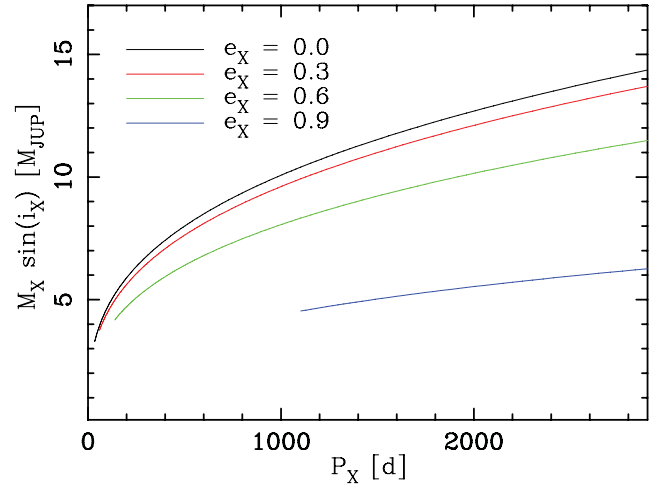


**Figure 7.** Limits for  $M_X \sin(i_X)$  for a putative fourth body estimated from our RV measurements, for several values of eccentricities. The value of the rms = 157  $\text{m s}^{-1}$  was assumed to be the RV semi-amplitude. The lower limit of the period is 35 d (the major semiaxis of 0.24 au) which refers to the shortest stable *circular* orbit (Holman & Wiegert 1999). For eccentric orbits the limits are terminated at the shortest periods having the distance of periastron larger than 0.24 au (around 60, 139 and 1107 d). Using  $i_X = 52.4^\circ$  increases the detection limits by about 26 per cent ( $1/\sin(52.4^\circ) \simeq 1.26$ ).

light is detected. It is not however excluded that the eccentricity of the perturber is very large which would allow more massive bodies in long-period orbits to induce the Kozai cycles and remain undetectable by the RVs. The component C discovered by Zuckerman et al. (1997) could be the perturbing body, but with relation (7) it seems that it is not very likely. For the estimated mass  $M_3 = 0.13 M_\odot$  the orbital eccentricity  $e_3$  would have to be larger than 0.98, assuming a fortunate but improbable case that the star is currently seen exactly at the apocentre, and  $\Omega_3 = 0^\circ$ ; thus  $a_3 [\text{au}] = 277/(1 + e_3)$ . For less fortunate cases the value of  $e_3$  would have to be even larger.

The other possibility is the presence of a putative fourth body reported in the *Hipparcos* catalogue. Boden & Lane (2001) inspected the available RV data in order to find a 114 d period predicted by the *Hipparcos* catalogue, and with a high level of confidence they excluded the existence of such a period in the spectroscopic data. With relation (6) we can show that if a body in a  $P_H = 114.02$  d circular orbit exists, it would have to have  $M_H \gtrsim 0.15 M_{\text{JUP}}$ . From Fig. 7 we can put an upper mass limit of  $5.44 M_{\text{JUP}}$ , taking into account the reported inclination of  $113.21^\circ$ , which itself is within the allowed limits. The reported major semi-axis of the *Hipparcos* photocentric orbital solution is  $a_{12,H} = 0.0515$  au (at the distance to BY Dra). Assuming the maximum mass ratio  $M_H/(M_1 + M_2) = 0.0035$ , the fourth body barycentric major semi-axis would be 16.07 au (after correcting for the inclination), but Kepler’s third law predicts the major semi-axis of 0.53 au for the given period and masses. Such a body would produce the RV signal much stronger than 157  $\text{m s}^{-1}$ . We can thus conclude that the *Hipparcos* solution is unrealistic.

## 7 SUMMARY

We present the most precise orbital and physical parameters of an important astrophysical object – the low-mass SB2 BY Dra, a prototype of an entire class of variable stars. We reach a level of precision which allows us to put important constraints on the nature of this object. We conclude that this is not a pre-main-sequence

system, despite its high orbital eccentricity and a possible spin–orbit misalignment. However, the gravitational influence of a fourth, yet undetected body in the system may explain the observed value of  $e$  and the spin–orbit alignment may be inferred from the available data if a value of the rotational velocity smaller than claimed in the literature is used. The observed rotational period and the eccentricity suggest that the BY Dra AB system is in the rotational equilibrium. However, if the observed eccentricity is indeed due to the presence of the fourth body, the putative companion may have its mass in the planetary regime. The whole dynamical and tidal picture of this system is more complicated than we previously thought and deserving perhaps a dedicated theoretical, observational and numerical analysis.

## ACKNOWLEDGMENTS

We would like to thank Professor Tsevi Mazeh for his *invaluable* comments and suggestions, and Arne Rau for carrying out the Keck I/HIRES observations in the years 2006–2007. The authors wish to recognize and acknowledge the very significant cultural role and reverence that the summit of Mauna Kea has always had within the indigenous Hawaiian community. We are most fortunate to have the opportunity to conduct observations from this mountain. This work benefits from the efforts of the PTI collaboration members who have each contributed to the development of an extremely reliable observational instrument. We thank PTI's night assistant Kevin Rykoski for his efforts to maintain PTI in excellent condition and operating PTI.

This research was cofinanced by the European Social Fund and the national budget of the Republic of Poland within the framework of the Integrated Regional Operational Programme, Measure 2.6. Regional innovation strategies and transfer of knowledge – an individual project of the Kuyavian–Pomeranian Voivodship ‘Scholarships for PhD students 2008/2009 – IROP’, and by the grant N N203 379936 from the Ministry of Science and Higher Education. Support for KGH is provided by Centro de Astrofísica FONDAP Proyecto 15010003, MK is supported by the Foundation for Polish Science through a FOCUS grant and fellowship and by the Polish Ministry of Science and Higher Education through grants N N203 005 32/0449 and N N203302035. MWM acknowledges support from the Townes Fellowship Programme, an internal UC Berkeley SSL grant, and the State of Tennessee Center of Excellence programme. This research was supported in part by the National Science Foundation under Grant No PHY05-51164. The observations on the TNG/SARG have been funded by the Optical Infrared Coordination network (OPTICON), a major international collaboration supported by the Research Infrastructures Programme of the European Commissions Sixth Framework Programme.

This research has made use of the Simbad database, operated at CDS, Strasbourg, France, and of data products from the Two Micron All Sky Survey, which is a joint project of the University of Massachusetts and the Infrared Processing and Analysis Center/California Institute of Technology, funded by the National Aeronautics and Space Administration and the National Science Foundation.

## REFERENCES

Barnes E. S., Evans D. S., Moffet T. J., 1978, MNRAS, 183, 285  
Bensby T., Feltzing S., Lundström I., 2003, A&A, 410, 527

Boden A. F., Lane B. F., 2001, ApJ, 547, 1071  
Boden A.F., 2000, in Lawson P. R., ed., Principles of Long Baseline Stellar Interferometry. JPL Publication, Pasadena, p. 9  
Bopp B. W., Evans D. S., 1973, MNRAS, 164, 343  
Bopp B. W., Noah P., Klimke A., 1980, AJ, 85, 1386  
Carpenter J. M., 2001, AJ, 121, 2851  
Chugainov P. S., 1966, Inf. Bull. Var. Stars, 122, 1  
Colavita M. M., 1997, ApJ, 510, 505  
Cristaldi S., Rodono M., 1968, Inf. Bull. Var. Stars, 252, 2  
Cristaldi S., Rodono M., 1970, A&AS, 2, 223  
Cristaldi S., Rodono M., 1971, A&A, 12, 152  
Cutri R. M. et al., 2003, The IRSA 2MASS All-Sky Catalog of Point Sources, NASA/IPAC Infrared Science Archive  
Demarque P., Woo J.-H., Kim Y.-C., Yi S. K., 2004, ApJS, 155, 667  
Devor J. et al., 2008, ApJ, 687, 1253  
Fabrycky D., Tremaine S., 2007, ApJ, 669, 1298  
Ford E., Kozinsky B., Rasio F. A., 2000, ApJ, 535, 385  
Głębocki R., Stawikowski A., 1995, Acta Astron., 45, 725  
Hełminiak K. G., Konacki M., 2011, A&A, 526, A29  
Hełminiak K. G. et al., 2011, A&A, 527, A14  
Holman M. J., Wiegert P. A., 1999, AJ, 117, 621  
Hut P., 1981, A&A, 99, 126  
Johnson D. R. H., Soderblom D. R., 1987, AJ, 93, 864  
Konacki M., 2009, in Pont F., Sasselov D., Holman M., eds, Proc. IAU Symp. 253, Transiting Planets. Cambridge Univ. Press, Cambridge, p. 141  
Konacki M., Muterspaugh M. W., Kulkarni S. R., Hełminiak K. G., 2009, ApJ, 704, 513  
Konacki M., Muterspaugh M. W., Kulkarni S. R., Hełminiak K. G., 2010, ApJ, 719, 1293  
Kozai Y., 1962, AJ, 67, 591  
Krzemiński W., 1969, in Kunar S., ed., Low Luminosity Stars. Gordon and Breach Publishing Co., London, p. 57  
Krzemiński W., Kraft R. P., 1967, AJ, 72, 307  
Kurucz R. L., 1995, in Adelman S. J., Wiese W. L., eds, ASP Conf. Ser. Vol. 78, Astrophysical Applications of Powerful New Databases. Astron. Soc. Pac., San Francisco, p. 205  
Lucke P. B., Mayor M., 1980, A&A, 92, 182  
Masani A., Broglia P., Pestarion E., 1955, Mem. Soc. Astron. Ital., 26, 183  
Mazeh T., 2008, in Goupil M.-J., Zahn J.-P., eds, EAS Publ. Ser. Vol. 29, Tidal Effects in Stars, Planets and Disks. EDP Sciences, Les Ulis, p. 1  
Mazeh T., Shaham J., 1979, A&A, 77, 145  
Münch G., 1944, ApJ, 99, 271  
Nordström B. et al., 2004, A&A, 418, 989  
Perryman M. A. C. et al., 1997, A&A, 323  
Pettersen B. R., Olah K., Sandmann W. H., 1992, A&AS, 96, 497  
Popper D. M., 1953, PASP, 65, 278  
Röser S., Schilbach E., Schwan H., Kharchenko N. V., Piskunov A. E., Scholz R.-D., 2008, A&A, 488, 401  
Strassmeier K. G., Hall D. S., Fekel F. C., Scheck M., 1993, A&AS, 100, 173  
Torres G., Andersen J., Giménez A., 2010, A&AR, 18, 67  
van de Kamp P., 1967, Principles of Astrometry. Freeman, San Francisco  
van der Bliek N. S., Manfroid J., Bouchet P., 1996, A&AS, 119, 547  
van Leeuwen F., 2007, A&A, 474, 653  
Vogt S. S., Fekel F., 1979, ApJ, 234, 958  
Wilson R. E., Devinney R. J., 1971, ApJ, 166, 605  
Yi S. K., Demarque P., Kim Y.-C., Lee Y.-W., Ree C. H., Lejeune T., Barnes S., 2001, ApJS, 136, 417  
Zahn J.-P., Bouchet L., 1989, A&A, 223, 112  
Zhao J., Zhao G., Chen Y., 2009, ApJ, 692, L113  
Zucker S., Mazeh T., 1994, ApJ, 420, 806  
Zuckerman B., Webb R. A., Becklin E. E., McLean I. S., Malkan M. A., 1997, AJ, 114, 805

This paper has been typeset from a  $\text{\TeX}/\text{\LaTeX}$  file prepared by the author.